Theory of cumulative small-angle collisions in plasmas

K. Nanbu
Institute of Fluid Science, Tohoku University, Sendai 980-77, Japan
(Received 30 September 1996; revised manuscript received 23 December 1996)

A succession of small-angle binary collisions can be grouped into a unique binary collision with a large scattering angle. The latter is called a cumulative collision. This makes it possible to treat the cumulative collision like a collision between neutral molecules. A significant feature of the cumulative collision is that the probability density function for a deflection angle depends on the time spent by a charged particle while engaged in the cumulative collision. Here a simple analytic expression for the function is proposed which is easy to use together with the Monte Carlo method. The validity of the present theory is ascertained by calculating various relaxation phenomena in plasmas. The theory is best suited to particle simulation of plasmas. [S1063-651X(97)04004-X]

PACS number(s): 52.20.Fs, 52.65.Pp, 02.70.Lq, 52.80.−s

I. INTRODUCTION

A recent trend in plasma-assisted materials processing is towards ''low gas density and high plasma density'' as seen in inductively coupled, electron cyclotron resonance, and helicon sources. The Coulomb collision between charged particles plays a more important role in such plasmas and the particle or kinetic approach to plasma modeling makes more sense than the fluid model approach. Here we propose a different theory on Coulomb collision in such plasmas. The theory is best suited to the particle simulation of dense plasmas. It can be applied to fully ionized plasma as it stands. For partially ionized plasma additional collisions should be taken into consideration. For example, argon plasma consists of four species such as A (ground state), A^* (metastable), A^+ (ion), and e^- (electron). There are ten types of collisions. We can treat $e^- - e^-$, $A^+ - A^+$, and $e^- - A^+$ collisions by the present theory, $e^- - A$ and $e^- - A^*$ collisions by the theory of Surendra, Graves, and Jellum [1], $A^+ - A$ and $A^+ - A^*$ by the theory of Nanbu and Kitatani [2], and $A - A$, $A - A^*$, and $A^* - A^*$ collisions by the direct simulation Monte Carlo method [3,4]. Every collision is governed by short-range force except the Coulomb collision. Note that even if a small-angle collision dominates in some short-range collision, the present theory is not applicable to it.

Electrostatic forces between charged particles have a much longer range than forces between neutral molecules. Although ''encounter'' is a more accurate word than ''collision'' in such a case, here we use ''collision.'' In the Coulomb collision, distant collisions with a small scattering angle are much more dominant than close collisions. The cumulative deflection angle of a particle is correctly treated by considering successive binary collisions with a small scattering angle [5,6]. Takizuka and Abé [7] first proposed a binary collision model suited to a Monte Carlo particle simulation of plasma. Their method, which faithfully mimics a Fokker-Planck operator, has been used in the particle-in-cell simulation of discharge plasma [8] and in the simulation of ionospheric plasma [9]. There are two points that can be improved in Takizuka and Abé's method. The first is that the collision rate (or frequency) depends on the various types of relaxation such as slowing down, energy transfer, and velocity deflection. Which shall we choose when some types of relaxation occur simultaneously? The second is the requirement that the time step should be much smaller than the relaxation time. This is necessary because in their method small-angle collisions are calculated one by one. However, the use of a small time step is often computationally intensive. In the binary collision theory presented here, these two problems are solved; a single collision rate is introduced for any relaxation phenomenon and a succession of small-angle binary collisions are grouped into a unique binary collision with a large scattering angle.

Much work has been published concerning the effect of electron-electron collision on the energy distribution function of the electron, e.g., Rochwood [10], Weng and Kushner [11], Hashiguchi [12], and Yousfi, Himoudi, and Gaouar [13]. (See also the references cited in [13].) The method to treat the Coulomb collision presented in this paper is quite different from these studies.

In Sec. II the mathematical formulation of the approach is given, a lengthy manipulation being described in the Appendix. This theory is applied to various standard problems in plasma physics in Sec. III. The numerical results show that the theory works well for all the cases examined in this paper.

II. THEORY

A. Cumulative scattering angle

Coulomb collisions in plasma can be treated as successive binary collisions [5]. We consider a charged particle which has undergone small-angle collisions N times in plasma. How large is the cumulative scattering angle? Surprisingly, there has been no theory on this angle. We start from the simplest case; a test particle is traversing among fixed field particles. Extension to the case of moving field particles is done later in Sec. II D. Let $\mathbf{g}_0$ be the initial velocity of the test particle, and $\mathbf{g}_1, \mathbf{g}_2, \ldots, \mathbf{g}_k, \ldots, \mathbf{g}_N$ be its first, second,..., Nth postcollision velocities. The cumulative scattering angle χ_N after N collisions is the angle between $\mathbf{g}_0$ and $\mathbf{g}_N$, i.e.,

$$\cos\chi_N = \mathbf{g}_0 \cdot \mathbf{g}_N / g^2, \tag{1}$$

where $g=|\mathbf{g}_0|$. Since the kinetic energy of the test particle does not change in collisions with fixed field particles, all g_k's are equal to g.

We introduce a Cartesian coordinate system (x,y,z) whose z axis is directed along $\mathbf{g}_0$. Let (θ_1,φ_1) be the polar and azimuthal angles of $\mathbf{g}_1$ in the system (x,y,z). Clearly the scattering angle χ_1 is equal to θ_1. Next we rotate the z axis by θ_1 in the plane $y=x\tan\varphi_1$ so that the new z axis coincides with $\mathbf{g}_1$. We label the new coordinate system (x_1,y_1,z_1). The z_1 axis is now in the direction of $\mathbf{g}_1$. We measure the direction (θ_2,φ_2) of $\mathbf{g}_2$ in the system (x_1,y_1,z_1). The cumulative scattering angle χ_2 is a function of $\theta_1,\theta_2,\varphi_1$, and φ_2. Rotation of the coordinate system as described above can be repeated as many times as required. Let (θ_k,φ_k) be the direction of $\mathbf{g}_k$ measured in the system $(x_{k-1},y_{k-1},z_{k-1})$. We then have

$$\sin^2\frac{\chi_N}{2}=\frac{1}{4}\sum_{k=1}^{N}\theta_k^2+\frac{1}{2}\sum_{k=2}^{N}\sum_{l=1}^{k-1}\theta_k\theta_l\cos(\varphi_k-\varphi_l). \quad (2)$$

A full derivation of Eq. (2) can be found in the Appendix. It is important, however, to mention here that this derivation assumes that $\theta_1,\theta_2,...,\theta_N\ll 1$, which is valid here because of small-angle scattering.

Clearly, (θ_1,φ_1), (θ_2,φ_2),..., are random variables. A statistical nature of successive small-angle collisions requires that $\theta_1,\theta_2,...,$ are mutually independent random variables which obey the same probability law. In addition the set $\{\theta_1,\theta_2,...\}$ is independent of the set $\{\varphi_1,\varphi_2,...\}$. Since the test particle has no preferred azimuthal direction, the angles $\varphi_1,\varphi_2,...,$ are uniformly distributed between 0 and 2π. We then have

$$\langle\cos(\varphi_k-\varphi_l)\rangle=\frac{1}{(2\pi)^2}\int_0^{2\pi}\int_0^{2\pi}\cos(\varphi_k-\varphi_l)d\varphi_k d\varphi_l=0,$$

where $\langle\ \rangle$ denotes the expectation. The expectation of Eq. (2) becomes

$$\left\langle\sin^2\frac{\chi_N}{2}\right\rangle=\frac{1}{4}\sum_{k=1}^{N}\langle\theta_k^2\rangle. \quad (3)$$

If we consider that (θ_1,φ_1), (θ_2,φ_2),..., are not random variables but their realizations, we have only to interpret $\langle\theta_k^2\rangle$ in Eq. (3) as an ensemble average, i.e., an average over a collection of many test particles. Since $\theta_1,\theta_2,...,$ obey the same probability law, we have $\langle\theta_1^2\rangle=\langle\theta_2^2\rangle=\ldots$. Then Eq. (3) reduces to

$$\left\langle\sin^2\frac{\chi_N}{2}\right\rangle=\frac{1}{4}\langle\theta_1^2\rangle N. \quad (4)$$

However, the applicability of Eq. (4) is limited; as $N\to\infty$, the right-hand side tends to infinity whereas the left-hand side should be smaller than unity. We need to add a correction to Eq. (4), which is described in Sec. II B.

B. Relaxation of $\langle\sin^2(\chi_N/2)\rangle$

It is expected that as the collision number N becomes very large, the scattering is isotropic, hence the probability density function of χ_N is $(\sin\chi_N)/2$. We then have

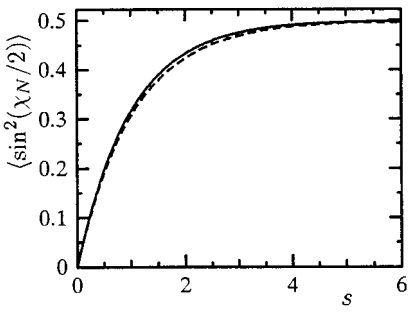

FIG. 1. Relaxation of $\langle\sin^2(\chi_N/2)\rangle$. Solid line shows Eq. (9) and dashed line shows the simulation.

$\langle\sin^2(\chi_N/2)\rangle=1/2$. To examine the approach to this limit, and also to find the probability density function of χ_N we simulated the stochastic process of χ_1, χ_2,..., by using the procedure in the Appendix. The deflection angle θ_k for kth small-angle collision is given by [14]

$$\tan\frac{\theta_k}{2}=\frac{|q_\alpha q_\beta|}{4\pi\epsilon_0\mu g^2 b}, \quad (5)$$

where q_α and q_β are the charges of the test particle and field particle, respectively, ϵ_0 is the permittivity of free space, μ is the mass of the test particle, and b is the impact parameter. As usual, the maximal value of b is set equal to the Debye length λ_D [5,6]. A random sample of b is given by $\lambda_D\sqrt{U}$, U being a random number uniformly distributed between 0 and 1. Substitution of this b into Eq. (5) yields

$$\theta_k=2\tan^{-1}\left(\frac{\theta_{\min}}{2\sqrt{U}}\right),$$

where $\theta_{\min}(=b_0/\lambda_D)$ is the minimal deflection angle of $\mathbf{g}_k$, and b_0 is $|q_\alpha q_\beta|/(2\pi\epsilon_0\mu g^2)$. The azimuthal angle φ_k is given by $2\pi U$, where U is another random number. Once (θ_k,φ_k) are given, we can obtain χ_k, as in the Appendix. The assumption that $\theta_1,\theta_2,...,$ are small is not used in the simulation. Note that $\theta_k\to\pi$ as $U\to 0$ but most of the random samples of θ_k are very small.

In this simulation the only free parameter is $\theta_{\min}$. Usually $\theta_{\min}$ is of order $e^{-10}(=2.6\times10^{-3}$ deg). However, to speed up the relaxation we choose larger $\theta_{\min}$. The simulation is performed for $\theta_{\min}=0.5$, 1, and 2 deg. The expectation $\langle\theta_1^2\rangle$ is given by

$$\langle\theta_1^2\rangle=8\int_0^1\left[\tan^{-1}\left(\frac{\theta_{\min}}{2\eta}\right)\right]^2\eta\,d\eta, \quad (6)$$

where the unit of $\theta_{\min}$ is radian. It is 3.051×10^{-3} for $\theta_{\min}=1$ deg. We have found that $\langle\sin^2(\chi_N/2)\rangle$ is a unique function of s defined by

$$s=\tfrac{1}{2}\langle\theta_1^2\rangle N, \quad (7)$$

irrespective of $\theta_{\min}$. This is true also for the probability density function mentioned later. Therefore, we hereafter give the results only for $\theta_{\min}=1$ deg. Figure 1 shows $\langle\sin^2(\chi_N/2)\rangle$ as a function of s. Here the ensemble average has been ob-

tained by the use of 200 000 test particles. The simulation data shows that relaxation of $\langle \sin^2(\chi_N/2)\rangle$ can be well represented by

$$\left\langle \sin^2 \frac{\chi_N}{2} \right\rangle = \frac{1}{2}(1-e^{-cs}), \tag{8}$$

where c is a constant. Let us determine the constant c theoretically. We can say that Eq. (4) is valid at least for small s. The constant c is thus determined by expanding the right-hand side of Eq. (8) for small s and equating the result to Eq. (4). This leads to one of the most important equations in the present theory

$$\left\langle \sin^2 \frac{\chi_N}{2} \right\rangle = \frac{1}{2}(1-e^{-s}). \tag{9}$$

We see from Fig. 1 that Eq. (9) is a good match.

C. Probability density function of χ_N

Let $f(\chi_N)d\Omega$ be the probability that $\mathbf{g}_N$ is scattered in the solid angle $d\Omega(=2\pi \sin\chi_N d\chi_N)$. We then have

$$2\pi \int_0^\pi f(\chi_N)\sin\chi_N d\chi_N = 1. \tag{10}$$

Here $2\pi f(\chi_N)\sin\chi_N$ is the probability density function for χ_N. For isotropic scattering $f(\chi_N)$ is $1/4\pi$. Let us find $f(\chi_N)$. In addition to Eq. (10) it should satisfy Eq. (9), i.e.,

$$2\pi \int_0^\pi f(\chi_N)\sin^2 \frac{\chi_N}{2} \sin\chi_N \, d\chi_N = \frac{1}{2}(1-e^{-s}). \tag{11}$$

In the numerical simulation of Sec. II B, the distribution of χ_N is examined by counting the number M_i of χ_N's in the interval (χ_{i-1},χ_i), where $\chi_i = i\Delta\chi (i=1,2,...,36)$ and $\Delta\chi = 5$ deg. The mean value of $f(\chi_N)$ in the ith interval is given by

$$f_i = \frac{M_i}{M\Omega_i},$$

where $M(=200\,000)$ is the total number of test particles and $\Omega_i[=2\pi(\cos\chi_{i-1}-\cos\chi_i)]$ is the solid angle (set to $\chi_{i-1}=0$ for $i=1$). The value of f_i is assigned to the weighted center $(\chi_i)_c$ of the ith interval, i.e.,

$$(\chi_i)_c = \frac{2\pi}{\Omega_i} \int_{\chi_{i-1}}^{\chi_i} \chi \sin\chi \, d\chi,$$

$$= 2\pi(\chi_{i-1}\cos\chi_{i-1} - \chi_i\cos\chi_i + \sin\chi_i - \sin\chi_{i-1})/\Omega_i.$$

The distribution of $\ln[f(\chi_N)]$, thus determined, is plotted in Fig. 2 as a function of $\cos\chi_N$ for $N=100$ to 3000. Note that the abscissa is from 1 to -1. As expected, $f(\chi_N)$ tends to $1/4\pi$ for large N. Based on the simulation data we introduce the simplest approximation that $\ln[f(\chi_N)]$ is a linear function of $\cos\chi_N$ for all N, i.e., $f(\chi_N) = B\exp(A\cos\chi_N)$, where A and B are the constants. Note that $\ln[f(\chi_N)]$ is approximately linear for all $\theta_{\min}$'s considered in this paper. It is most probable that this linearity is kept for any $\theta_{\min}$. The constant B is given as a function of A by use of the normalizing condition Eq. (10). Now we have

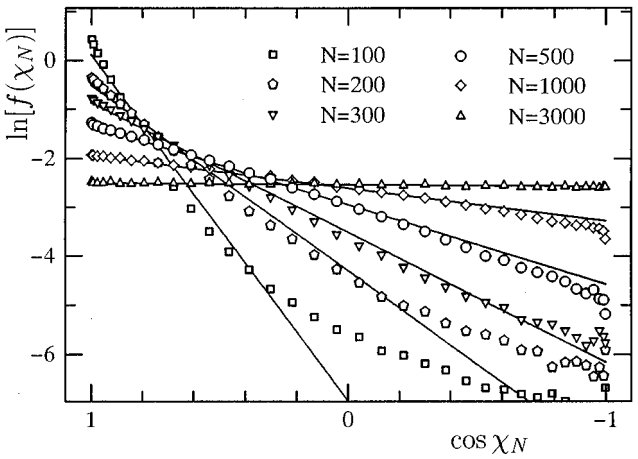

FIG. 2. Probability density of deflection angle. Plots show the simulation and solid lines show Eq. (12).

$$f(\chi_N) = \frac{A}{4\pi \sinh A}\exp(A\cos\chi_N). \tag{12}$$

Substitution of Eq. (12) into Eq. (11) yields

$$\coth A - A^{-1} = e^{-s}. \tag{13}$$

Once the number N of small-angle collisions is given, s is known. We find A by solving Eq. (13). Then $f(\chi_N)$, hence the probability density function $F(\chi_N)[\equiv 2\pi f(\chi_N)\sin\chi_N]$ of χ_N can be obtained.

We soon see that Eq. (12) works well in various applications. Some remarks on Eqs. (12) and (13) are given here. We have found from some sample calculations that the value of A should be accurate, otherwise the development of the physical system depends on the time step employed. This is explained later. The value of A for a given s can be easily obtained by use of Newton's method [15]. In applications it is better to prepare a table of $A(s)$ in advance and use interpolation to obtain the value of A for an arbitrary s. Table I is a part of such a table. The interval of s in our full table is 0.001. Beyond the tabulated values of s we set $A = 1/s$ for

TABLE I. Values of $A(s)$.

s	A	s	A
0.01	100.5	0.3	3.845
0.02	50.50	0.4	2.987
0.03	33.84	0.5	2.448
0.04	25.50	0.6	2.067
0.05	20.50	0.7	1.779
0.06	17.17	0.8	1.551
0.07	14.79	0.9	1.363
0.08	13.01	1	1.207
0.09	11.62	2	0.4105
0.1	10.51	3	0.1496
0.2	5.516	4	0.054 96

$s<0.01$ and $A=3e^{-s}$ for $s>3$. The error is only 0.5% for the former and 0.15% for the latter. The value of A is very large for small s, hence small values of χ_N make the greatest contribution to $f(\chi_N)$. Since $\cos\chi_N \simeq 1-\chi_N^2/2$, we see that for small s the function $f(\chi_N)$ has a Gaussian profile with a narrow width. This is reasonable since for small s the test particle is hardly deviated from its original direction. For large s, the value of A is very small, hence $f(\chi_N)\simeq 1/4\pi$ as stated before. Thus we call s the isotropy parameter.

We have to rewrite Eq. (7) for practical applications. If the maximal impact parameter is $b_{\max}$, which is set equal to λ_D, the number N of small-angle collisions in time Δt is

$$N=n_\beta g \pi b_{\max}^2 \Delta t, \tag{14}$$

where n_β is the number density of field particles. The analytic approximation of $\langle\theta_1^2\rangle$ defined by Eq. (6) is [14]

$$\langle\theta_1^2\rangle = 2\left(\frac{b_0}{b_{\max}}\right)^2 \ln\Lambda, \tag{15}$$

where $\Lambda=\lambda_D/b_0$. By the use of Eqs. (14) and (15), Eq. (7) takes the form

$$s=n_\beta g \pi b_0^2\ (\ln\Lambda)\Delta t. \tag{16}$$

Since no restrictive condition is imposed on the magnitude of s, the choice of Δt is arbitrary. However, if we want to examine a relaxation process of some physical system, s should be small, otherwise the system reaches the final state after only one time step.

Let us denote χ_N by χ. In determining postcollision velocity we need a random sample of $\cos\chi$. This can be easily obtained from $F(\chi)$, i.e.,

$$\cos\chi = \frac{1}{A}\ln(e^{-A}+2U\sinh A), \tag{17}$$

where U is the random number. Since $0<\chi<\pi$, we have $\sin\chi=(1-\cos^2\chi)^{1/2}$. The value of A is large for small s and an exponential overflow occurs. To avoid this we replace Eq. (17) by $\cos\chi=1+s\ln U$. For $s>6$ the scattering is almost isotropic, so that we can replace Eq. (17) by $\cos\chi=2U-1$.

D. Moving field particles

The speeds $g_0, g_1, g_2, \ldots$, of the test particle are equal in the case of fixed field particles. However, when the field particles are moving, we have to consider the relative velocity $\mathbf{g}(=\mathbf{v}_\alpha-\mathbf{v}_\beta)$, where $\mathbf{v}_\alpha$ and $\mathbf{v}_\beta$ are the velocities of the test particle and its collision partner in the field, respectively. After the first small-angle collision the initial relative velocity $\mathbf{g}_1(=\mathbf{v}_{\alpha 1}-\mathbf{v}_{\beta 1})$ is scattered by θ_1 and becomes $\mathbf{g}_1'(=\mathbf{v}_{\alpha 1}'-\mathbf{v}_{\beta 1}')$. Since we consider the elastic collision, g_1' is equal to g_1. Next let us consider the second small-angle collision of the test particle. Since the collision partner is not the same, the precollision relative velocity $\mathbf{g}_2(=\mathbf{v}_{\alpha 2}-\mathbf{v}_{\beta 2})$ is not equal to $\mathbf{g}_1'$ where $\mathbf{v}_{\alpha 2}=\mathbf{v}_{\alpha 1}'$ and $\mathbf{v}_{\beta 2}$ is the velocity of the second partner. The vector $\mathbf{g}_2$ is deflected by θ_2 and becomes $\mathbf{g}_2'(=\mathbf{v}_{\alpha 2}'-\mathbf{v}_{\beta 2}')$ after the collision. As before $g_2'=g_2$ but $g_2\neq g_1$. Similarly, after the third collision $\mathbf{g}_3(=\mathbf{v}_{\alpha 3}-\mathbf{v}_{\beta 3})$ becomes $\mathbf{g}_3'(=\mathbf{v}_{\alpha 3}'-\mathbf{v}_{\beta 3}')$, where $\mathbf{v}_{\alpha 3}=\mathbf{v}_{\alpha 2}'$ and $\mathbf{v}_{\beta 3}$ is the precollision velocity of the third partner. Until the end of the third collision, the relative velocity changes in the order of $\mathbf{g}_1$, $\mathbf{g}_1'$, $\mathbf{g}_2$, $\mathbf{g}_2'$, $\mathbf{g}_3$, and $\mathbf{g}_3'$. The changes $\mathbf{g}_1'\rightarrow\mathbf{g}_2$ and $\mathbf{g}_2'\rightarrow\mathbf{g}_3$ are irrelevant to collision. Our concern is in the cumulative deflection angle due to small-angle collisions; we disregard the changes $\mathbf{g}_1'\rightarrow\mathbf{g}_2, \mathbf{g}_2'\rightarrow\mathbf{g}_3, \ldots$, in calculating the deflection angle. Further repetition of this procedure shows that Eq. (2) also holds in the case of moving field particles. However, we should note that θ_k depends on $g_k(=|\mathbf{v}_{\alpha k}-\mathbf{v}_{\beta k}|)$ as well as the impact parameter b. See Eq. (5), where g is to be replaced by g_k. (Recall that θ_k depends only on the impact parameter in the case of fixed field particles.) Equation (3) also holds for moving field particles. Averaging θ_k^2 over b, we have for the same reasoning that led to Eq. (15)

$$\langle\theta_k^2\rangle = 2\left(\frac{b_0}{b_{\max}}\right)^2 \ln\Lambda. \tag{18}$$

Here $b_0=|q_\alpha q_\beta|/(2\pi\epsilon_0\mu_{\alpha\beta}g_k^2)$ and $\mu_{\alpha\beta}=m_\alpha m_\beta/(m_\alpha+m_\beta)$, m_α and m_β being the masses of the test and field particles, respectively. The expectation $\langle\theta_k^2\rangle$ changes from collision to collision, so that Eq. (4) needs to be reinterpreted; $\langle\theta_1^2\rangle$ in Eq. (4) is actually the average $\overline{\langle\theta^2\rangle}$ of $\langle\theta_1^2\rangle$, $\langle\theta_2^2\rangle, \ldots, \langle\theta_N^2\rangle$. We approximate this average simply by $\langle\theta_1^2\rangle$. Then Eq. (4) holds as it stands. For a single test particle the approximation $\overline{\langle\theta^2\rangle}\simeq\langle\theta_1^2\rangle$ may be poor. However, in practical simulations we consider an ensemble of test particles. The value of $\langle\theta_1^2\rangle$ for each test particle is expected to fluctuate around $\overline{\langle\theta^2\rangle}$, so that replacing $\overline{\langle\theta^2\rangle}$ by $\langle\theta_1^2\rangle$ has little effect on the ensemble averaged data.

Let us consider N small-angle collisions in Δt. We have from Eq. (7)

$$s=\frac{\ln\Lambda}{4\pi}\left(\frac{q_\alpha q_\beta}{\epsilon_0\mu_{\alpha\beta}}\right)^2 n_\beta g^{-3}\Delta t, \tag{19}$$

where $g=g_1$. Since $\ln\Lambda$ depends only weakly on g, we replace it, as usual, by $\ln\Lambda=\ln(\lambda_D/\langle b_0\rangle)$, where $\langle b_0\rangle=|q_\alpha q_\beta|/(2\pi\epsilon_0\mu_{\alpha\beta}\langle g^2\rangle)$. The expectation $\langle g^2\rangle$ is equal to $3kT/\mu_{\alpha\beta}$ if plasma is in equilibrium at temperature T.

Let g be the relative speed and $\mathbf{v}_\alpha$ be the velocity of a test particle at time t. The procedure to determine the velocity at $t+\Delta t$ is summarized as follows: (1) Make a random sample of the field particle velocity $\mathbf{v}_\beta$ by the use of the field velocity distribution function and calculate $\mathbf{g}(=\mathbf{v}_\alpha-\mathbf{v}_\beta)$, and hence s from Eq. (19). (2) Determine A from Eq. (13) and obtain $\cos\chi$ from Eq. (17). (3) The velocity $\mathbf{v}_\alpha'$ after a cumulative collision is given by [16]

$$\mathbf{v}_\alpha' = \mathbf{v}_\alpha - \frac{m_\beta}{m_\alpha+m_\beta}[\mathbf{g}(1-\cos\chi)+\mathbf{h}\sin\chi], \tag{20a}$$

$$\mathbf{v}_\beta' = \mathbf{v}_\beta + \frac{m_\alpha}{m_\alpha+m_\beta}[\mathbf{g}(1-\cos\chi)+\mathbf{h}\sin\chi], \tag{20b}$$

where $\mathbf{g}=\mathbf{v}_\alpha-\mathbf{v}_\beta$ and the Cartesian components of $\mathbf{h}$ are

$$h_x = g_\perp \cos\varepsilon,$$

$$h_y = -(g_y g_x \cos\varepsilon + g g_z \sin\varepsilon)/g_\perp,$$

$$h_z = -(g_z g_x \cos\varepsilon - g g_y \sin\varepsilon)/g_\perp.$$

Here $g_\perp = (g_y^2 + g_z^2)^{1/2}$ and $\varepsilon = 2\pi U$, U being a random number. We added Eq. (20b) because in some cases the field particles are the collection of test particles itself. If $m_\beta \gg m_\alpha$, the change in $\mathbf{v}'_\beta - \mathbf{v}_\beta$ is of order m_α/m_β.

Repeating the three stages described above for all test particles and advancing time stepwise, we can determine macroscopic properties of the ensemble at any time.

E. Multicomponent plasma

The procedure described in the preceding section can be generalized to the case when plasma consists of many charged species α, β, γ, ... It may be enough to consider a ternary mixture of α, β, and γ. We have to consider $\alpha-\beta$, $\beta-\gamma$, α-γ collisions between unlike species in addition to $\alpha-\alpha$, $\beta-\beta$, $\gamma-\gamma$ collisions between like species. Let N_α, N_β, and N_γ be the number of sample particles in a reference cell. (The sample particles are random samples taken out of real particles.) For simplicity we set $N_\alpha = N_\beta = N_\gamma (= N)$ and N is assumed even.

Let $\{\mathbf{v}_{\alpha i}, \mathbf{v}_{\beta i}, \mathbf{v}_{\gamma i};\ i = 1,\ldots,N\}$ be the velocities of sample particles at time t. New velocities $\{\mathbf{v}'_{\alpha i}, \mathbf{v}'_{\beta i}, \mathbf{v}'_{\gamma i};\ i = 1,\ldots,N\}$ at time $t + \Delta t$ can be determined by calculating $\alpha-\beta$, $\beta-\gamma$, $\alpha-\gamma$, $\alpha-\alpha$, $\beta-\beta$, and $\gamma-\gamma$ collisions in turn. The order of collisions is arbitrary. Let us replace g in Eq. (19) by $g(\alpha i, \beta j)[\equiv |\mathbf{v}_{\alpha i} - \mathbf{v}_{\beta j}|]$ and s by $s_{\alpha\beta}$. The procedure is as follows.

(i) Make N pairs $(\mathbf{v}_{\alpha i}, \mathbf{v}_{\beta j})$: Pick up randomly a vector $\mathbf{v}_{\beta j}$ one by one from all $\mathbf{v}_{\beta j}$'s without replacement and set them in array. Then the first, second,..., are the partners of $\mathbf{v}_{\alpha 1}$, $\mathbf{v}_{\alpha 2}$,... . Obtain $g(\alpha i, \beta j)$ and, hence, $s_{\alpha\beta}$ for each pair. Determine A from Eq. (13) and obtain $\cos\chi$ from Eq. (17). The postcollision velocities $(\mathbf{v}'_{\alpha i}, \mathbf{v}'_{\beta j})$ are given by Eq. (20).

(ii) Make N pairs $(\mathbf{v}_{\beta i}, \mathbf{v}_{\gamma j})$ and determine postcollision velocities as in stage (i). Note that precollision velocities $\mathbf{v}_{\beta i}$ in this stage are postcollision velocities of stage (i).

(iii) Make N pairs $(\mathbf{v}_{\alpha i}, \mathbf{v}_{\gamma j})$ and determine postcollision velocities. In this stage, precollision velocities $\mathbf{v}_{\alpha i}$ and $\mathbf{v}_{\gamma j}$ are postcollision velocities in stage (i) and stage (ii), respectively. Hereafter, precollision velocities should be always postcollision velocities of previous stages.

(iv) Make $N/2$ pairs $(\mathbf{v}_{\alpha i}, \mathbf{v}_{\alpha j})$: Set all $\mathbf{v}_{\alpha i}$'s randomly in array, as in the array of $\mathbf{v}_{\beta j}$'s in stage (i). Then pick up two by two to make $N/2$ pairs. Obtain $g(\alpha i, \alpha j)$ and, hence, $s_{\alpha\alpha}$, A, and $\cos\chi$ for each pair. The postcollision velocities are given by Eq. (20), where we set $\beta = \alpha$.

(v) Make $N/2$ pairs $(\mathbf{v}_{\beta i}, \mathbf{v}_{\beta j})$ and obtain postcollision velocities as in stage (iv).

(vi) Obtain postcollision velocities of $N/2$ pairs $(\mathbf{v}_{\gamma i}, \mathbf{v}_{\gamma j})$ as in stage(iv).

We see that every particle collides three times in Δt, twice with unlike particles and once with like particles, e.g., it is $\alpha-\beta$, $\alpha-\gamma$, and $\alpha-\alpha$ collisions for particle α. The unlike collisions result in momentum and energy exchange between two species and like collisions promote equilibration in each species. The total number of collisions in plasma with three species is $3\times N + 3\times(N/2) = (S/2)\times N_T$ where $S(=3)$ is the number of species and $N_T(=3N)$ is the total number of sample particles. The total collision number is in general given by $SN_T/2$ when $N_\alpha = N_\beta = N_\gamma = \cdots = N$. In successful particle simulation the total collision number is to be proportional to N_T. After discovery of a similar collision algorithm for neutral gases the particle simulation of rarefied gas flows advanced drastically [3,4]. As for how to make collision pairs in the case of $N_\alpha \neq N_\beta \neq N_\gamma$,..., see Takizuka and Abé [7].

III. APPLICATIONS

In the particle simulation of rarefied gas flows the flow field is divided into small cells and molecular collisions are treated independently in each cell [3,4]. This is reasonable because the cell size is chosen to be nearly equal to the mean free path. Similarly, in the particle-in-cell simulation of plasma the computational domain is divided into cells to calculate the electric and/or magnetic field [8]. Since the cell size is of the same order as the Debye length, Coulomb collisions can be treated independently in each cell. When plasma is spatially nonuniform, we have to consider the motion of particles in addition to collisions. Here we apply the theory described in the preceding section to spatially uniform plasmas. Most of the example problems are taken from Refs. [6] and [7].

A. Thermalization of electron beams in plasma

Suppose that an electron beam with speed $v_{\alpha 0}$ is directed in the z direction at time $t = 0$. Here we consider only the collisions of beam electrons with field particles. We begin with the case of fixed field particles, i.e., $m_\beta = \infty$ and $\mathbf{v}_\beta = 0$. The expectations (or ensemble averages) $\langle \hat{v}_z \rangle$ and $\langle \hat{v}_\perp^2 \rangle$ in the early stage are [5]

$$\langle \hat{v}_z \rangle = 1 - \hat{t}, \tag{21a}$$

$$\langle \hat{v}_\perp^2 \rangle = 2\hat{t}. \tag{21b}$$

Here the symbols with a caret are nondimensional. They are obtained by dividing velocity by $v_{\alpha 0}$ and time by τ_0, where

$$\frac{1}{\tau_0} = \frac{n_\beta q_\alpha^2 q_\beta^2 \ln\Lambda}{8\pi\sqrt{2}\,\epsilon_0^2 m_\alpha^{1/2} \varepsilon_{\alpha 0}^{3/2}},$$

$\varepsilon_{\alpha 0}$ being $m_\alpha v_{\alpha 0}^2/2$. We have $s = \Delta\hat{t}$ from Eq. (16). Figure 3 shows $\langle \hat{v}_z \rangle$ and $\langle \hat{v}_\perp^2 \rangle$. The simulation data are obtained for $\Delta\hat{t} = 0.05$ and $N_\alpha = 10^5$. They agree well with Eqs. (21a) and (21b) at small $\hat{t}$. Since the Maxwellian distribution holds for $\mathbf{v}_\alpha$ as $\hat{t} \to \infty$, we have $\langle \hat{v}_\perp^2 \rangle \to 2/3$ as $\hat{t} \to \infty$. This is satisfied by the simulation data. We have ascertained that the numerical solution does not depend on $\Delta\hat{t}$; the solutions for $\Delta\hat{t} = 0.01$, 0.1, and 1 were indistinguishable from that for $\Delta\hat{t} = 0.05$.

The next example is the thermalization of a beam in an electron gas. Let the energy of the electron beam, $\varepsilon_{\alpha 0}$ be 100 eV, with the field electrons always in equilibrium at a constant temperature $kT_\beta = 2$ eV, k being the Boltzmann constant. The solutions for small $\hat{t}$ are [6]

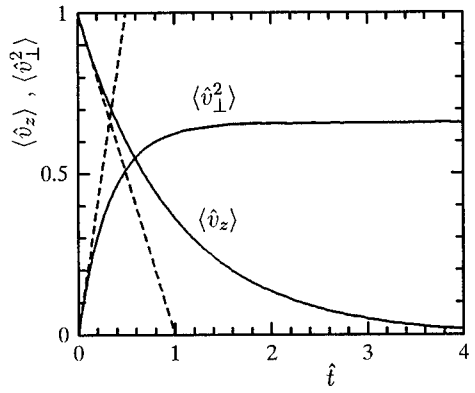

FIG. 3. Relaxation of $\langle \hat{v}_z \rangle$ and $\langle \hat{v}_\perp^2 \rangle$ in fixed field particles. Solid lines show the simulation and dashed lines show Eq. (21).

$$\langle \hat{v}_z \rangle = 1 - 2\hat{t}, \tag{22a}$$

$$\langle \hat{v}_\perp^2 \rangle = (2 - \eta_{\alpha\beta}^{-1})\hat{t}, \tag{22b}$$

where $\eta_{\alpha\beta} = \varepsilon_{\alpha 0}/kT_\beta = 50$. In equilibrium we have $\langle \hat{v}_\perp^2 \rangle = \eta_{\alpha\beta}^{-1} = 0.02$. This shows that $\langle \hat{v}_\perp^2 \rangle$ should be maximal at some $\hat{t}$. The isotropy parameter s becomes $s = 4\hat{g}^{-3}\Delta\hat{t}$, where $\hat{g} = |\hat{\mathbf{v}}_\alpha - \hat{\mathbf{v}}_\beta|$. The time step $\Delta\hat{t}$ can be estimated by the use of mean $\hat{g}$ in equilibrium. Our choice is $\Delta\hat{t} = 0.01$. Figure 4 shows the numerical results for $\langle \hat{v}_z \rangle$ and $\langle \hat{v}_\perp^2 \rangle$. Agreement with Eqs. (22a) and (22b) is good at small $\hat{t}$. In addition, $\langle \hat{v}_\perp^2 \rangle \to 0.02$ for large $\hat{t}$, which is the equilibrium value.

The third example is the beam thermalization in equilibrium argon plasma. Now there are two kinds of field particles, field electrons (β) and ions (β'). We set the field temperature as $kT_\beta = 2$ eV and $kT_{\beta'} = 0.02$ eV. The small-time solutions are [6]

$$\langle \hat{v}_z \rangle = 1 - 3\hat{t}, \tag{23a}$$

$$\langle \hat{v}_\perp^2 \rangle = (4 - \eta_{\alpha\beta}^{-1})\hat{t}, \tag{23b}$$

where $\eta_{\alpha\beta} = 50$ as before and $\ln\Lambda$ for $\alpha - \beta$ and $\alpha - \beta'$ collisions are assumed equal. The numerical solutions for $\Delta\hat{t} = 0.01$ are in Fig. 5. They agree well with Eqs. (23a) and (23b).

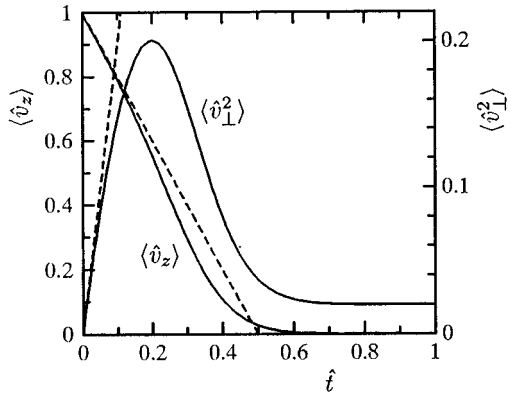

FIG. 4. Relaxation of $\langle \hat{v}_z \rangle$ and $\langle \hat{v}_\perp^2 \rangle$ in electron gas. Solid lines show the simulation and dashed lines show Eq. (22).

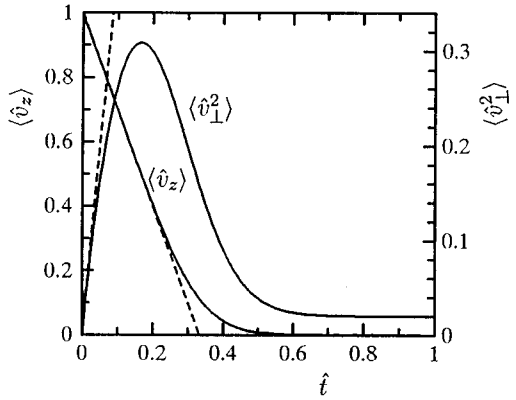

FIG. 5. Relaxation of $\langle \hat{v}_z \rangle$ and $\langle \hat{v}_\perp^2 \rangle$ in argon plasma. Solid lines show the simulation and dashed lines show Eq. (23).

B. Relaxation of the velocity distribution function

We consider the relaxation of an electron gas due to $e-e$ collisions. There is no need to distinguish the test and field particles. The velocity distribution is assumed to be initially an ellipsoidal one with temperatures $T_x \neq T_y = T_z$. The overall electron temperature $T_e (= \frac{1}{3}T_x + \frac{2}{3}T_y)$ is constant since the kinetic energy is conserved for the system. The reference time τ_0 is defined by

$$\frac{1}{\tau_0} = \frac{n_e e^4 \ln\Lambda}{8\pi\sqrt{2}\,\epsilon_0^2 m_e^{1/2}(kT_e)^{3/2}}, \tag{24}$$

where e is the electronic charge. The analytic solution for $\Delta T (= T_x - T_y)$ is [6,7]

$$\Delta T = (\Delta T)_0 \exp\left(-\frac{8}{5\sqrt{2\pi}}\,\hat{t} \right),$$

where $(\Delta T)_0$ is ΔT at $t = 0$ and $\hat{t} = t/\tau_0$. The solution is obtained based on the assumption $|\Delta T| \ll T_x$. We choose $T_x = 1.3T_y$ at $t = 0$ so that the assumption may be satisfied approximately. The analytic solutions for T_x/T_e and T_y/T_e are shown by the dashed lines in Fig. 6. The simulation solutions are obtained by using 10^6 sample electrons. The time step is $\Delta\hat{t} = 0.02$. The initial velocities of electrons are sampled from the ellipsoidal distribution. A set of these velocities is slightly corrected so that there may be no flow and the temperatures T_x, T_y, T_z determined from 10^6 samples may coincide with the initial temperatures. The solid lines in Fig. 6 show the simulation solutions. They agree fairly well with the analytic solutions.

C. Relaxation of electron flow in field ions

At $t = 0$ the velocity distribution function of electron, f, is assumed to be the Maxwellian distribution with a flow in the x direction.

$$f(\mathbf{v}) = (2\pi R_e T_e)^{-3/2} \exp\left[-\frac{(\mathbf{v} - \hat{\mathbf{i}}V)^2}{2R_e T_e} \right], \tag{25}$$

where $R_e = k/m_e$, T_e is the electron temperature, $\mathbf{v}$ is the velocity, V is the flow velocity, and $\hat{\mathbf{i}}$ is the unit vector in the

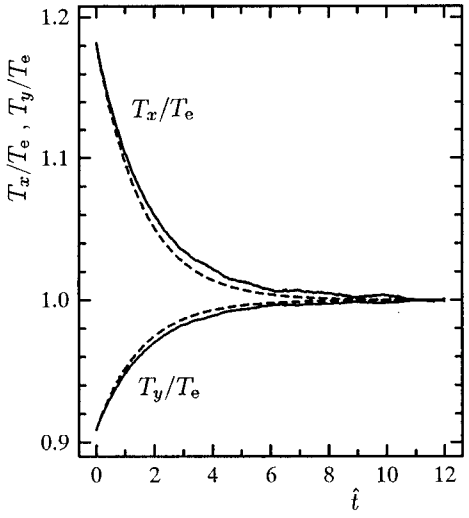

FIG. 6. Relaxation of temperature components. Solid lines show the simulation and dashed lines show the solution of the relaxation equation.

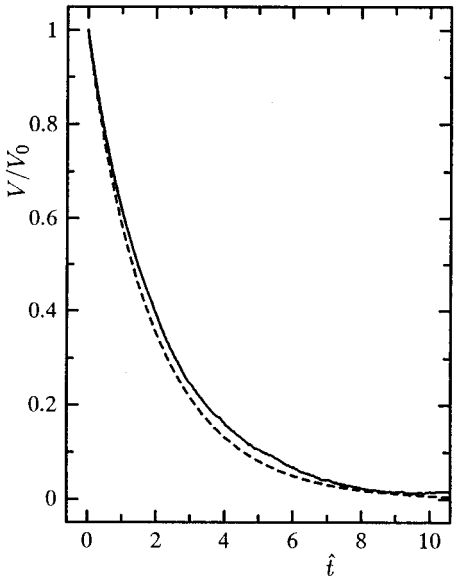

FIG. 7. Relaxation of flow velocity. Solid line shows the simulation and dashed line shows the solution of Eq. (26).

x direction. We set $T_e=T_0$ and $V=V_0$ at $t=0$. The relaxation equation for V is obtained for small t [7]. We extend the equation to the case of arbitrary t. It is

$$\frac{dV}{d\hat{t}}=-\left(\frac{kT_0}{\varepsilon_f}\right)^{3/2}\mu\left(\frac{\varepsilon_f}{kT_e}\right)V, \tag{26}$$

where $\varepsilon_f=m_eV^2/2$, $\hat{t}=t/\tau_{00}$, and $\mu(x^2)$ is defined by

$$\mu(x^2)=\mathrm{erf}x-\frac{2}{\sqrt{\pi}}xe^{-x^2}.$$

Here τ_{00} is τ_0 in Eq. (24) for $T_e=T_0$, n_e being replaced by ion density n_i.

We compare the simulation solution with the solution of Eq. (26). Before starting the simulation all conditions on which Eq. (26) is based should be clarified. These are as follows: (a) The velocity distribution of electron is subject to Eq. (25) at any time. (b) The velocity distribution of ion is independent of time and is given by the Maxwellian distribution with no flow. (c) Only $e-i$ collisions are taken into consideration, $e-e$ collisions being disregarded. (d) $m_e/m_i \ll 1$ and $(m_i/m_e)(\varepsilon_e/kT_i) \gg 1$, where m_i is the mass of ion, T_i is the temperature of ion, and ε_e is the kinetic energy of electron. The particle simulation should be performed in such a way that all these conditions are satisfied. Note that even if $f(\mathbf{v})$ is initially Maxwellian, it is not so during relaxation.

Let the previously arbitrary ions be protons $(m_i=1836m_e)$ and set $T_i=T_0$ and $\varepsilon_{f0}(=m_eV_0^2/2)=kT_0/2$. Since the energy relaxation time for $e-i$ collision is much larger than the momentum relaxation time, the mean energy $\langle\varepsilon_e\rangle$ is almost constant during the relaxation of the flow velocity V, i.e.,

$$\langle\varepsilon_e\rangle=\tfrac{3}{2}kT_e+\tfrac{1}{2}m_eV^2=\tfrac{3}{2}kT_0+\tfrac{1}{2}m_eV_0^2.$$

This equation is used to eliminate T_e in Eq. (26). The dashed line in Fig. 7 is the solution of Eq. (26) obtained by the use of the Runge-Kutta-Gill method. Note that the second part of condition (d) is well satisfied for $\varepsilon_e=\langle\varepsilon_e\rangle$.

Initial velocities of electrons are sampled from Eq. (25) for $T_e=T_0$ and $V=V_0$. The ion velocities are also sampled from the Maxwellian distribution for $T_i=T_0$. Let N_e and N_i be the numbers of sample electrons and ions. Our choice is $N_e=N_i=10^5$. Since N_e is finite, the flow velocity and temperature determined from the set of sample velocities show a slight deviation from the given values. The sample velocities are corrected so as to make the deviation null. A similar correction is also done for the ion velocities. As for ions, the initial set of velocities are used at any time. The isotropy parameter s of Eq. (16) takes the form

$$s=\left(\frac{m_e}{\mu_{ei}}\right)^2\hat{g}^{-3}\Delta\hat{t},$$

where μ_{ei} is the reduced mass and $\hat{g}$ is the relative speed between an electron and ion pair, made dimensionless by dividing by $(2kT_0/m_e)^{1/2}$. The time step $\Delta\hat{t}$ is 0.04. The collision pair is determined by the method described in Sec. II E. The velocity distribution of electrons at the end of time step $\hat{t}=\Delta\hat{t}$ does not have the form of Eq. (25). To satisfy condition (a) we first determine V and T_e from a set of velocities at $\hat{t}=\Delta\hat{t}$ and then replace the set by a new set of velocities sampled from Eq. (25). A slight correction is done for the new set in the same way as was done for the initial set. These procedures are repeated at the end of each time step. The solid line in Fig. 7 shows V/V_0 obtained from the simulation. Agreement with the solution of Eq. (26) is good.

D. Equilibration of electron and ion temperatures

Let T_e and T_i be the electron temperature and ion temperature, respectively. Suppose that $T_e \neq T_i$ at $t=0$. Equili-

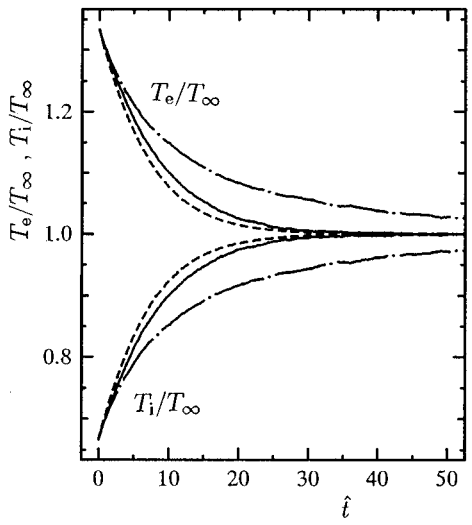

FIG. 8. Equilibration of electron and ion temperatures. Solid lines show the simulation, dashed lines show the solution of the relaxation equation, and dashed-dotted lines show simulation in which the condition of temporal Maxwellian distribution is not used.

bration of temperatures is described by the relaxation equation for $\Delta T(=T_e-T_i)$ [5,6]. In the case of $n_e=n_i$ energy conservation requires

$$T_e+T_i=T_{e0}+T_{i0}=2T_\infty,$$

where T_{e0} and T_{i0} are the initial temperatures and T_∞ is the final equilibrium temperature. The relaxation equation is based on the assumption that the electrons and the ions always have Maxwellian distributions with different temperatures T_e and T_i. This should be incorporated in the particle simulation. To increase the relaxation rate we consider an ion with imaginary mass such as $m_i=4m_e$. The initial condition is $T_{e0}=2T_{i0}$. The dashed lines in Fig. 8 show T_e/T_∞ and T_i/T_∞ obtained from the relaxation equation. The $e-i$ collisions are simulated by the present method. The isotropy parameter s is

$$s=\hat{g}^{-3}\Delta\hat{t},$$

where $\hat{g}=g/v_{\rm ref}$, $v_{\rm ref}=(kT_\infty/\mu_{ei})^{1/2}$, $\Delta\hat{t}=\Delta t/\tau_{\rm ref}$, and

$$\frac{1}{\tau_{\rm ref}}=\frac{n_e e^4\ln\Lambda}{4\pi\epsilon_0^2\mu_{ei}^{1/2}(kT_\infty)^{3/2}}.$$

In this problem the energies of both electrons and ions show relaxation owing to $e-i$ collisions. Equation (19) shows that s is symmetrical with respect to exchange of α and β. This symmetry should be kept when we nondimensionalize g and Δt in s. We see that $v_{\rm ref}$ and $\tau_{\rm ref}$ satisfy this condition. The simulation is performed for $\Delta\hat{t}=0.25$ and $N_e=N_i=10^5$. Initial velocities of electrons and ions are sampled from Maxwellian distributions with temperatures T_{e0} and T_{i0}. These velocities are slightly corrected so that there may exist no flow and sample averages may yield the given T_{e0} and T_{i0} exactly. The temperatures T_e and T_i at $\hat{t}=\Delta\hat{t}$ are obtained from the velocities of electrons and ions. By use of these temperatures new velocities at $\hat{t}=\Delta\hat{t}$ are sampled from Maxwellian distributions with T_e and T_i and are corrected as before. The solid lines in Fig. 8 indicate the simulation solution. It shows a fairly good agreement with the solution of the relaxation equation. The dashed-dotted lines are the results obtained by assuming Maxwellian distributions only $t=0$. We see that in fact the velocity distributions are not Maxwellian during the relaxation process.

E. Drift velocity of electrons in an oscillating electric field

In the previous examples there are no external forces. Here we consider the case when plasma is in an oscillating electric field. Time is advanced step by step as before. We have to consider both acceleration and collision of particles in each time step. This is treated separately; first acceleration is calculated and then collision is taken into account. We consider the plasma in a typical fusion condition. It consists of electrons and deuterons. The number densities and temperatures are $n_e=n_i=10^{21}/\mathrm{m}^3$ and $kT_e=kT_i=1$ keV. Initially the plasma is in equilibrium. The Debye length λ_D for electron is 7.4×10^{-6} m. The impact parameter $\langle b_0\rangle$ for $e-e$ and $e-i$ collisions is the same and is given by $e^2/(6\pi\epsilon_0 kT_e)$, hence $\ln\Lambda=15.9$. The isotropy parameter s for $e-e$ and $e-i$ collisions can be obtained from Eq. (19). Ions are insensitive to the electric field. We suppose that the ions always have a Maxwellian velocity distribution with the initial temperature; thus acceleration of ions and $i-i$ collisions are disregarded. An oscillating electric field $E\cos\omega t$ in the x direction is switched on at $t=0$. If there is no collision, the drift velocity $\langle v\rangle$ of electrons in the x direction is

$$\langle v\rangle=\langle v_0\rangle-\frac{eE}{m_e\omega}\sin\omega t,$$

where v_0 is the initial velocity of electron and $\langle v_0\rangle\simeq0$. Since the time average of $\langle v\rangle$ over a period is almost zero, we consider the time average of $\langle v\rangle^2$, i.e.,

$$\overline{\langle v\rangle^2}=\langle v_0\rangle^2+\tfrac{1}{2}V^2\simeq\tfrac{1}{2}V^2 \tag{27}$$

where $V=eE/m_e\omega$. Here we examine the effect of $e-e$ and $e-i$ collisions on $\overline{\langle v\rangle^2}$. We fix V at $V=\sqrt{8kT_e/\pi m_e}$ for any E and ω.

The time step is determined as follows. For $e-e$ collisions Eq. (19) gives $s\sim2\times10^6\Delta t$, where we used $g^{-3}\sim\langle g^3\rangle^{-1}=(\sqrt{\pi}/32)(m_e/kT_e)^{3/2}$. Our choice is $\Delta t=2.5\times10^{-7}$ s, for which $s\sim0.5$. The simulation is performed for $0<t<50t_p$, where $t_p(=f^{-1}=2\pi/\omega)$ is the period. The frequency f is varied from 1 kHz to 1 MHz. A period is divided into J time steps, e.g., $J=400$ for $f=10$ kHz. The time point t_j in the nth cycle is $t_j=(n-1)t_p+(j-1)\Delta t$ $(j=1,2,\ldots,J)$. Let $(v_i)_j$ be the velocity of ith electron at time t_j. This is changed by the electric field to

$$v_i(t)=(v_i)_j-V(\sin\omega t-\sin\omega t_j),$$

where $t_j<t<t_{j+1}$. The ensemble average is

$$\langle v(t)\rangle=\langle v\rangle_j-V(\sin\omega t-\sin\omega t_j).$$

Next we obtain

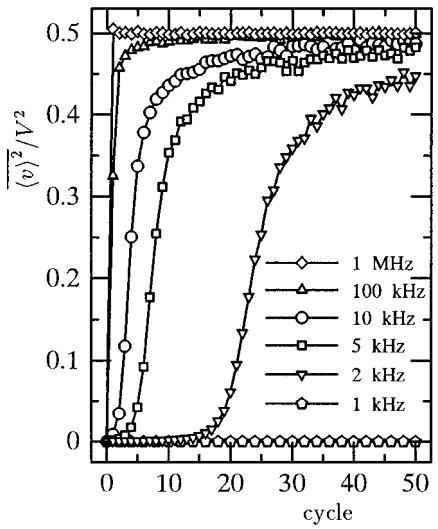

FIG. 9. Relaxation of square of electron drift velocity in an oscillating electric field.

$$I_j=\int_{t_j}^{t_{j+1}}\langle v(t)\rangle^2 dt.$$

After this we calculate all $e-e$ collisions and subsequently all $e-i$ collisions. Similarly, I_{j+1} is obtained by the use of the postcollision velocity $(v_i)_{j+1}$. The time average for the nth cycle is given by

$$\overline{\langle v\rangle^2}=(I_1+I_2+\cdots+I_J)/t_p\,.$$

Figure 9 shows $\overline{\langle v\rangle^2}/V^2$ as a function of cycle n. The numbers of samples are $N_e=N_i=10^5$. At $f=1$ MHz the Coulomb collisions have no effect on the drift velocity whereas the drift disappears at $f=1$ kHz owing to the Coulomb collisions. We can see relaxation in the case of $f=100$ kHz, 10 kHz, 5 kHz, and 2 kHz. The steady state values of $\overline{\langle v\rangle^2}$ for $f=10$ kHz, 5 kHz, and 2 kHz appear to be smaller than that of Eq. (27).

IV. CONCLUSION

The treatment of Coulomb collisions in plasmas has been greatly simplified by grouping a succession of small-angle binary collisions into a unique binary collision with a large scattering angle. The main results are expressed in analytic forms.

(1) The procedure to determine the velocity of a particle at the end of a time step Δt is as follows.

(i) First the isotropy s is calculated at the beginning of time step:

$$s=n_\beta g\pi b_0^2(\ln\Lambda)\Delta t,$$

where $b_0[=|q_\alpha q_\beta|/(2\pi\epsilon_0\mu_{\alpha\beta}g^2)]$ is the impact parameter.

(ii) For a given s we determine the constant A from the equation

$$\coth A-A^{-1}=e^{-s}.$$

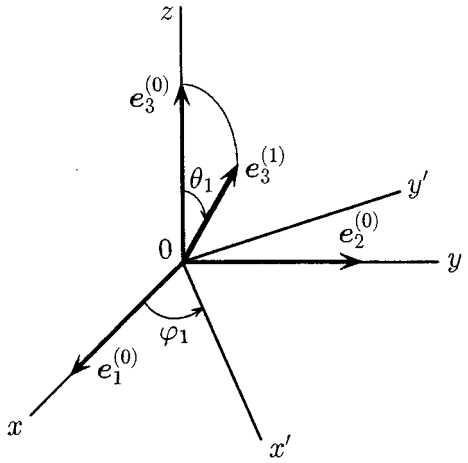

FIG. 10. Coordinate system rotation.

(iii) The probability $f(\chi)d\Omega$ that the postcollision relative velocity is scattered in solid angle $d\Omega(=2\pi\sin\chi d\chi)$ is given by

$$f(\chi)d\Omega=\frac{A}{4\pi\,\sinh A}\,e^{A\cos\chi}d\Omega.$$

(2) We have applied this theory to various situations occurring in plasmas. In particular:

(i) Thermalization of electron beams in fields consisting of fixed field particles, an electron gas, and a nonequilibrium argon plasma.

(ii) Relaxation of electron gas due to $e-e$ collisions.

(iii) Relaxation of electron flow in field ions.

(iv) Equilibration of electron and ion temperatures.

(v) The drift velocity of electrons in an oscillating electric field.

The theory developed in this paper enabled us to reproduce analytical results for (i) to (iv) previously obtained by other authors with a high degree of accuracy.

(3) Clearly, development of a theory of cumulative collision has the potential for application in many fields involving plasma physics and plasma processing. By its very nature it enables the results of many small-angle collisions to be calculated extremely efficiently reducing computational costs.

ACKNOWLEDGMENTS

Calculations are carried out by the use of the SX-3R at the Computer Center of Tohoku University. The present work is supported by the Japan Atomic Energy Research Institute (Kansai Research Establishment) as a part of Advanced Laser System Research.

APPENDIX: CUMULATIVE SCATTERING ANGLE

We consider the rotation of the Cartesian coordinate system. See Fig. 10. When the z axis is turned by θ_1 in the zOx' plane, the new set of fundamental vectors in the Cartesian system is

$$\boldsymbol{e}_i^{(1)}=A_{ij}^{(1)}\boldsymbol{e}_j^{(0)}, \tag{A1}$$

where we used the repeated-subscript notation for summation. The matrix $A_{ij}^{(1)}$ is an abbreviation of

$$A(\theta_1,\varphi_1)=\begin{bmatrix} \cos\theta_1\cos^2\varphi_1+\sin^2\varphi_1 & (\cos\theta_1-1)\sin\varphi_1\cos\varphi_1 & -\sin\theta_1\cos\varphi_1 \\ (\cos\theta_1-1)\sin\varphi_1\cos\varphi_1 & \cos\theta_1\sin^2\varphi_1+\cos^2\varphi_1 & -\sin\theta_1\sin\varphi_1 \\ \sin\theta_1\cos\varphi_1 & \sin\theta_1\sin\varphi_1 & \cos\theta_1 \end{bmatrix}.$$

Equation (A1) can be obtained as follows. First the system $Oxyz$ is rotated by φ_1 around the z axis. The resulting system $Ox'y'z'$ is rotated by θ_1 around the y' axis to yield the system $Ox''y''z''$. The z'' axis is in the direction of $\mathbf{e}_3^{(1)}$. When the system $Ox''y''z''$ is rotated by $-\varphi_1$ around the z'' axis, we have the system whose fundamental vectors are given by Eq. (A1). If we regard $\mathbf{e}_3^{(0)}$ as $\mathbf{g}_0/g$ and $\mathbf{e}_3^{(1)}$ as $\mathbf{g}_1/g$, then $\theta_1(=\chi_1)$ is the scattering angle. Similarly we turn $\mathbf{e}_3^{(1)}$ and make $\mathbf{e}_3^{(2)}(=\mathbf{g}_2/g)$ whose polar and azimuthal angles measured in the $\mathbf{e}_1^{(1)}\mathbf{e}_2^{(1)}\mathbf{e}_3^{(1)}$ system are θ_2 and φ_2. The fundamental vectors are now

$$\mathbf{e}_i^{(2)}=A_{ij}^{(2)}\mathbf{e}_j^{(1)}, \tag{A2}$$

where the matrix $A^{(2)}$ denotes $A(\theta_2,\varphi_2)$. Substitution of Eq. (A1) into Eq. (A2) yields

$$\mathbf{e}_i^{(2)}=B_{ij}^{(2)}\mathbf{e}_j^{(0)}, \tag{A3}$$

where $B^{(2)}=A^{(2)}A^{(1)}$. Once θ_1,φ_1 and θ_2,φ_2 are given, the matrix $B^{(2)}$ is known. Clearly, $B_{31}^{(2)}$, $B_{32}^{(2)}$, and $B_{33}^{(2)}$ are the components of $\mathbf{e}_3^{(2)}$ in the $\mathbf{e}_1^{(0)}\mathbf{e}_2^{(0)}\mathbf{e}_3^{(0)}$ system. The polar angle χ_2 and azimuthal angle ψ_2 of $\mathbf{e}_3^{(2)}$ can be obtained from

$$\sin\chi_2\cos\psi_2=B_{31}^{(2)}, \tag{A4a}$$

$$\sin\chi_2\sin\psi_2=B_{32}^{(2)}, \tag{A4b}$$

$$\cos\chi_2=B_{33}^{(2)}. \tag{A4c}$$

If we use χ_2 and ψ_2, we can rewrite Eq. (A3) as

$$\mathbf{e}_i^{(2)}=[A(\chi_2,\psi_2)]_{ij}\mathbf{e}_j^{(0)}. \tag{A5}$$

The angle χ_2 is the cumulative scattering angle due to two collisions. The angle χ_3 after the third collision can be obtained as follows. Let θ_3 and φ_3 be the polar and azimuthal angles of $\mathbf{e}_3^{(3)}(=\mathbf{g}_3/g)$ in the $\mathbf{e}_1^{(2)}\mathbf{e}_2^{(2)}\mathbf{e}_3^{(2)}$ system, i.e.,

$$\mathbf{e}_i^{(3)}=A_{ij}^{(3)}\mathbf{e}_j^{(2)}=B_{ij}^{(3)}\mathbf{e}_j^{(0)}, \tag{A6}$$

where $B^{(3)}=A^{(3)}A(\chi_2,\psi_2)$, and Eq. (A5) is used. Now we can obtain the polar angle χ_3 and azimuthal angle ψ_3 of $\mathbf{e}_3^{(3)}$ from Eq. (A4) where χ_2, ψ_2, and $B^{(2)}$ are to be replaced by χ_3, ψ_3, and $B^{(3)}$. Repetition of this procedure gives $\chi_4,\chi_5,\ldots$. This procedure is used in Sec. II B in calculating cumulative scattering angle χ_N.

An analytic expression of χ_N can be derived if $\theta_1,\theta_2,\ldots$, are small. Our concern is $\mathbf{e}_3^{(n)}$, so that we introduce the simpler notations as

$$\hat{\mathbf{g}}_n(=\mathbf{g}_n/g)\equiv\mathbf{e}_3^{(n)},$$

$$G_i^{(n)}\equiv A_{3i}^{(n)}=(\sin\theta_n\cos\varphi_n,\sin\theta_n\sin\varphi_n,\cos\theta_n).$$

The extension of Eqs. (A2) and (A3) is

$$\mathbf{e}_i^{(n)}=A_{ij}^{(n)}\mathbf{e}_j^{(n-1)}, \quad (n=1,2,\ldots). \tag{A7}$$

We have from this equation

$$\begin{aligned}\hat{\mathbf{g}}_n&=G_i^{(n)}\mathbf{e}_i^{(n-1)},\\ &=G_i^{(n)}[A^{(n-1)}A^{(n-2)}\ldots A^{(1)}]_{ij}\mathbf{e}_j^{(0)}.\end{aligned} \tag{A8}$$

The cumulative scattering angle χ_n is given by

$$\begin{aligned}\cos\chi_n&=\mathbf{e}_3^{(0)}\cdot\hat{\mathbf{g}}_n\\ &=G_i^{(n)}[A^{(n-1)}A^{(n-2)}\ldots A^{(1)}]_{i3}.\end{aligned} \tag{A9}$$

If $O(\theta_n^3)$ and higher orders are disregarded in the expression of $A^{(n)}[=A(\theta_n,\varphi_n)]$, we have

$$A^{(n)}=I+\theta_nC^{(n)}-\tfrac{1}{2}\theta_n^2D^{(n)}, \tag{A10}$$

where I is the unit matrix and

$$C^{(n)}=\begin{pmatrix} 0 & 0 & -\xi_n \\ 0 & 0 & -\eta_n \\ \xi_n & \eta_n & 0 \end{pmatrix},$$

$$D^{(n)}=\begin{pmatrix} \xi_n^2 & \xi_n\eta_n & 0 \\ \xi_n\eta_n & \eta_n^2 & 0 \\ 0 & 0 & 1 \end{pmatrix},$$

with $\xi_n=\cos\varphi_n$ and $\eta_n=\sin\varphi_n$. From Eq. (A10) we obtain

$$\begin{aligned}A^{(n-1)}A^{(n-2)}\ldots A^{(1)}=I&+\sum_{k=1}^{n-1}\theta_kC^{(k)}-\frac{1}{2}\sum_{k=1}^{n-1}\theta_k^2D^{(k)}\\ &+\sum_{k=2}^{n-1}\sum_{l=1}^{k-1}\theta_k\theta_lC^{(k)}C^{(l)}.\end{aligned} \tag{A11}$$

On the other hand, for small θ_n we have

$$G_i^{(n)}=(\theta_n\xi_n,\theta_n\eta_n,1-\tfrac{1}{2}\theta_n^2). \tag{A12}$$

Substitution of Eqs. (A11) and (A12) into Eq. (A9) and some manipulation yields Eq. (2) in the text. Note that the first order terms disappear.

[1] M. Surendra, D. B. Graves, and G. M. Jellum, Phys. Rev. A **41**, 1112 (1990).
[2] K. Nanbu and Y. Kitatani, J. Phys. D. **28**, 324 (1995).
[3] G. A. Bird, *Molecular Gas Dynamics* (Clarendon, Oxford, 1976).
[4] K. Nanbu, in *Proceedings of the Fifteenth International Symposium on Rarefied Gas Dynamics*, edited by V. Boffi and C. Cercignani (Teubner, Stuttgart, 1986), Vol. 1, p. 369.
[5] L. Spitzer, Jr., *Physics of Fully Ionized Gases*, 2nd ed. (Interscience, New York, 1967).
[6] B. A. Trubnikov, *Reviews of Plasma Physics* (Consultants Bureau, New York, 1965), Vol. 1, p. 105.
[7] T. Takizuka and H. Abé, J. Comput. Phys. **25**, 205 (1977).
[8] C. K. Birdsall, IEEE Trans. Plasma Sci. **19**, 65 (1991).
[9] G. R. Wilson, J. L. Horwitz, and J. Lin, J. Geophys. Res. **97**, 1109 (1992).
[10] S. D. Rockwood, Phys. Rev. A **8**, 2348 (1973).
[11] Y. Weng and M. J. Kushner, Phys. Rev. A **42**, 6192 (1990).
[12] S. Hashiguchi, IEEE Trans. Plasma Sci. **19**, 297 (1991).
[13] M. Yousfi, A. Himoudi, and A. Gaouar, Phys. Rev. A **46**, 7889 (1992).
[14] M. A. Lieberman and A. J. Lichtenberg, *Principles of Plasma Discharges and Materials Processing* (Wiley, New York, 1994).
[15] R. G. Stanton, *Numerical Methods for Science and Engineering* (Maruzen, Tokyo, 1961), p. 84.
[16] W. G. Vincenti and C. H. Kruger, Jr., *Introduction to Physical Gas Dynamics* (Wiley, New York, 1967), p. 352.